Approaching the ultimate limits of communication efficiency with a photon-counting detector

Baris Erkmen, Bruce Moision, Samuel J. Dolinar, Kevin M. Birnbaum, Dariush Divsalar
Jet Propulsion Laboratory
California Institute of Technology
Pasadena, CA, 91109, USA
Email: baris.erkmen@jpl.nasa.gov

***Abstract*—Coherent states achieve the Holevo capacity of a pure-loss channel when paired with an optimal measurement, but a physical realization of this measurement is as of yet unknown, and it is also likely to be of high complexity. In this paper, we focus on the photon-counting measurement and study the photon and dimensional efficiencies attainable with modulations over classical- and nonclassical-state alphabets. We first review the state-of-the-art coherent on-off-keying (OOK) with a photon-counting measurement, illustrating its asymptotic inefficiency relative to the Holevo limit. We show that a commonly made Poisson approximation in thermal noise leads to unbounded photon information efficiencies, violating the conjectured Holevo limit. We analyze two binary-modulation architectures that improve upon the dimensional versus photon efficiency tradeoff achievable with conventional OOK. We show that at high photon efficiency these architectures achieve an efficiency tradeoff that differs from the best possible tradeoff—determined by the Holevo capacity—by only a constant factor. The first architecture we analyze is a coherent-state transmitter that relies on feedback from the receiver to control the transmitted energy. The second architecture uses a single-photon number-state source.**

I. Introduction

Electromagnetic waves are fundamentally governed by the laws of quantum mechanics, and, as such, when fields at optical wavelengths are used as the carrier in a communications system, the rates of reliable communication are determined by the Holevo capacity [1]. Although it is known that coherent states achieve the Holveo capacity when coupled with an optimal measurement, a physical realization of such a receiver is not yet known. The highest photon efficiency systems that have been demonstrated to date utilize on-off-keying (OOK) and a photon-counting receiver, see, e.g., [2], [3], [4], [5], [6]. Although alternative architectures have been proposed that theoretically exceed the performance of OOK+photon-counting, they require a large increase in complexity in return for a small gain [7], [8], [9]. This has motivated us to investigate the performance limits of photon-counting receivers.

In this paper we characterize the gap between conventional OOK+photon-counting and the Holevo limit, and illustrate the performance of two novel schemes to reduce that gap. The first utilizes a coherent-state transmitter that relies on feedback from the receiver to the transmitter to shut off the transmitted pulse once a photon is detected. The second uses a binary modulation consisting of vacuum and a single-photon number state. The first architecture can be viewed as a method to emulate the statistics of a single-photon number state at the receiver, which is near-optimal at large photon efficiencies. The latter architecture starts with a number-state modulation, but is sensitive to losses in the propagation path, and approaches the Holevo capacity only in the near field when the transmitter-to-receiver coupling is high.

We characterize the performance of these communications systems by their efficiency in utilizing available resources to transmit information. The resources of interest are the transmitted power and the bandwidth occupancy, or, more generally, the number of dimensions (temporal, spatial, or polarization) occupied by the signal. Let $\bar{n}_s$ denote the mean photon cost per channel use, D the dimensional cost per channel use (the number of dimensions required to span the collection of possible transmitted symbols per channel use), and $C(\bar{n}_s, D)$ the channel *capacity*, the maximum rate of information transmission, in bits per channel use. We define the photon information efficiency (PIE) as

$$i_p = \frac{C}{\bar{n}_s} \text{ (bits/photon)}$$

and the dimensional information efficiency (DIE) as

$$i_d = \frac{C}{D} \text{ (bits/dimension)}$$

and we denote the bound on the achievable pairs (i_p, i_d) by

$$c_d(i_p) = \max_{\bar{n}_s, D | C(\bar{n}_s, D)/\bar{n}_s = i_p} i_d$$

In this paper we focus on the behavior of c_d at large i_p.

II. Preliminaries

Here we review the formulation that converts free-space propagation into a set of beamsplitter channels. Quasi-monochromatic, paraxial propagation in vacuum through finite transmitter and receiver apertures is represented by a linear superposition integral given by

$$\hat{E}_L(\boldsymbol{\rho}, t) = \int_{\mathcal{A}_T} h(\boldsymbol{\rho} - \boldsymbol{\rho}')\hat{E}_0(\boldsymbol{\rho}', t - L/c)\mathrm{d}\boldsymbol{\rho}' + \hat{\mathcal{L}}_v(\boldsymbol{\rho}, t)$$

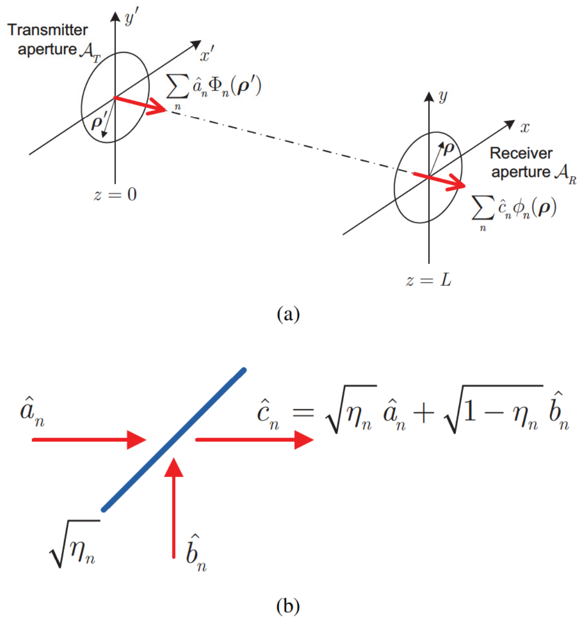

Fig. 1. The normal-mode decomposition for quasimonochromatic, paraxial free-space (i.e., vacuum) propagation. (a) The paraxial link geometry and propagation of eigenmodes, and (b) the beamsplitter representation of a single channel.

where $\hat{E}_0(\boldsymbol{\rho}, t)$ for $\boldsymbol{\rho} \in \mathcal{A}_T$ is the baseband envelope of a z-propagating $\sqrt{\text{photons/m}^2\text{s}}$-units quantum field operator transmitted from the $z = 0$ aperture, $\hat{E}_L(\boldsymbol{\rho}, t)$ for $\boldsymbol{\rho} \in \mathcal{A}_R$ is the corresponding quantum field operator received over the $z = L$ aperture, and $\hat{\mathcal{L}}_v(\boldsymbol{\rho}, t)$ is an auxiliary operator in its vacuum (i.e., unexcited) state needed to preserve the delta-function commutator brackets of the field operators.[1] The propagation kernel is the well-known Huygens-Fresnel Green's function from classical paraxial optics, namely

$$h(\boldsymbol{\rho} - \boldsymbol{\rho}') \equiv \frac{1}{i\lambda_0 L} e^{i2\pi L/\lambda_0} e^{i\pi|\boldsymbol{\rho}-\boldsymbol{\rho}'|^2/(\lambda_0 L)}$$

Because paraxial propagation is a linear transformation of the input field, a singular-value decomposition can be carried out to represent the propagation as a set of parallel (orthogonal) pure-loss channels, as shown in Fig. 1 [10], [11]. This decomposition—also known as the normal-mode decomposition [10], [11], [12]—results in a set of input eigenfunctions, $\{\Phi_n(\boldsymbol{\rho}')\}$, that are complete and orthonormal over the input aperture $\boldsymbol{\rho}' \in \mathcal{A}_T$. Upon propagation to the receiver plane, each input eigenfunction $\Phi_n(\boldsymbol{\rho}')$ is transformed into a corresponding output eigenfunction $\phi_n(\boldsymbol{\rho})$—where $\{\phi_n(\boldsymbol{\rho})\}$ also collectively form a complete and orthonormal basis on the receiver aperture $\boldsymbol{\rho} \in \mathcal{A}_R$—and is attenuated by a less-than-unity singular-value $\sqrt{\eta_n}$ due to diffraction. The resultant propagation model for the transmitter-plane field operator describing each input mode is therefore equivalent to that through a beamsplitter with photon-flux transmissivity η_n [10].

[1]The paraxial field operators satisfy $[\hat{E}_z(\boldsymbol{\rho}_1, t_1), \hat{E}_z^\dagger(\boldsymbol{\rho}_2, t_2)] = \delta(\boldsymbol{\rho}_1 - \boldsymbol{\rho}_2)\delta(t_1 - t_2)$ and $[\hat{E}_z(\boldsymbol{\rho}_1, t_1), \hat{E}_z(\boldsymbol{\rho}_2, t_2)] = 0$ for any $0 \le z \le L$ [10].

An optical communication system's link geometry can be classified into two regimes, according to the distribution of the singular values of its normal-mode decomposition. In the *far field* regime there is only one eigenfunction (i.e., η_1) whose power coupling differs appreciably from 0. In contrast, in the *near field* regime multiple η_n's are close to unity. For paraxial propagation in vacuum, whether a particular link geometry is in the far field or near field is determined solely by the Fresnel number product

$$D_F \equiv \frac{A_T A_R}{(\lambda_0 L)^2} = \sum_{n=1}^{\infty} \eta_n \tag{1}$$

where $D_F \ll 1$ corresponds to the *far field*, and $D_F \gg 1$ corresponds to the *near field*. In (1), A_T is the transmitter aperture area, A_R is that of the receiver aperture, λ_0 is the center wavelength of the optical field, and L is the distance between the transmitter and the receiver.

III. Ultimate Limits

In the remainder of this paper we focus on a single mode of these parallel channels, which is modeled as a beamsplitter with transmissivity η. On the pure-loss channel, and in the absence of background radiation, the bound on achievable pairs (i_p, c_d) is given by the *Holevo* limit,

$$\begin{aligned} i_p^{\text{Hol}} &= g(\bar{n}_s)/\bar{n}_s \\ c_d^{\text{Hol}} &= \bar{n}_s i_p^{\text{Hol}} \end{aligned} \tag{2}$$

where $g(x) = (1+x)\log_2(1+x) - x\log_2(x)$, and $\bar{n}_s$ is the mean photon number coupled to the receiver. The Holevo limit is achievable with coherent states and an optimal measurement. We are interested in particular in the behavior for $i_p^{\text{Hol}} \gg 1$. In this regime we have [8]

$$c_d^{\text{Hol}} \approx e i_p 2^{-i_p} \tag{3}$$

which represents the ultimate achievable efficiency at large i_p.

Let $(i_p^{\text{Hol}}(n_b), c_d^{\text{Hol}}(n_b))$ denote the ultimate efficiencies of the pure-loss channel in the presence of background radiation with mean photon number n_b. It has been shown that [13]

$$i_p^{\text{Hol}}(n_b) \ge (g(\bar{n}_s + n_b) - g(n_b))/\bar{n}_s \tag{4}$$

$$c_d^{\text{Hol}}(n_b) \ge i_p^{\text{Hol}}(n_b)\bar{n}_s \tag{5}$$

and it is conjectured that (4),(5) are met with equality [14]. We will take this conjecture to be true in the remainder. $i_p^{\text{Hol}}(n_b)$ increases with $1/\bar{n}_s$ at large $i_p^{\text{Hol}}(n_b)$. For $\bar{n}_s \ll n_b$ we have

$$\begin{aligned} i_p^{\text{Hol}}(n_b) &= \log_2(1 + 1/n_b) + o(\bar{n}_s)/\bar{n}_s \\ &\xrightarrow[\bar{n}_s \to 0]{} \log_2(1 + 1/n_b) \end{aligned} \tag{6}$$

Hence $i_p^{\text{Hol}}(n_b)$ is bounded.

In the following sections we examine the performance of a number of modulation and receiver architectures relative to the Holevo limits.

IV. Conventional On-Off Keying (OOK) with Coherent States

We first consider coherent-state on-off-keying (OOK) modulation paired with an ideal photon counting receiver. Implementations of this architecture have achieved the largest photon efficiencies demonstrated to date. It will also serve as a baseline for the systems that follow.

The OOK photon-counting channel is modeled as follows. In a channel use, a slot of duration of T seconds, we transmit either a pulse with photon flux equal to λ (expressed in units of photons/sec) with probability p, or no pulse—i.e., a photon flux equal to 0—with probability $1-p$. The mean photon cost per channel use is $\bar{n}_s = p\lambda T$. The bandwidth utilization may be taken to be $B = 1/T$, such that the dimensional cost of a channel use, the time-bandwidth product, is $BT = 1$. The photon flux is incident on an ideal infinite-bandwidth photon-counting photodetector. We consider the case where the signal is received in the absence or presence of background noise separately.

A. Noiseless Reception

In the absence of background, the output of the photodetector is a Poisson point process with rate either λ or 0, depending on the transmitted symbol. Since detection of a single photon is sufficient to unambiguously resolve the transmitted symbol, the channel output may be classified into a binary outcome: either no detection event occurs or at least one detection event occurs. This channel is a Z-channel, illustrated in Fig. 2, with $\epsilon = 1-e^{-\lambda T}$ the probability that at least one photon is detected given that the incident photon flux is λ.

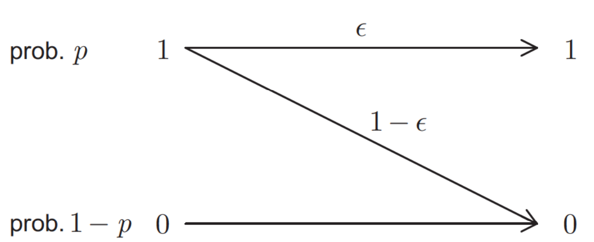

Fig. 2. The input-output probability transition map for a Z channel with erasure probability $1-\epsilon$.

The photon and dimensional efficiencies of this channel are given by [15]

$$i_p^{\text{OOK}} = \frac{h_2(\bar{n}_s) - h_2(\epsilon)}{d(\epsilon)}$$
$$i_d^{\text{OOK}} = \bar{n}_s d(\epsilon) i_p^{\text{OOK}}$$

where

$$h_2(\bar{n}_s) = -\log_2(\bar{n}_s) - \left(\frac{1-\bar{n}_s}{\bar{n}_s}\right)\log_2(1-\bar{n}_s)$$

and

$$d(\epsilon) = \frac{-\ln(1-\epsilon)}{\epsilon}$$

Let

$$c_d^{\text{OOK}}(i_p) = \max_{\bar{n}_s,\epsilon | i_p^{\text{OOK}} = i_p} i_d^{\text{OOK}} \tag{7}$$

At large i_p, we have[2]

$$c_d^{\text{OOK}} \approx \frac{2}{\ln(2)e} 2^{-i_p} \tag{8}$$

hence, from (3),

$$\frac{c_d^{\text{Hol}}(i_p)}{c_d^{\text{OOK}}(i_p)} \approx 2.561 i_p$$

at large i_p, and conventional OOK achieves a DIE that has *suboptimal* parametric dependence on PIE, relative to the optimal tradeoff predicted by the Holevo bound. In particular, the gap between the optimal DIE and that achieved by standard OOK grows linearly with increasing PIE.

B. Thermal Noise

Suppose now the signal is received in the presence of multi-mode thermal noise, with K noise modes coupling into the photodetector, each with variance N. The count statistic of non-pulsed and pulsed slots are, respectively, [16]

$$p_0(k;K) = \binom{K+k-1}{k}\left(\frac{1}{1+N}\right)^K \left(\frac{N}{1+N}\right)^k$$
$$p_1(k;K) = \frac{N^k}{(1+N)^{k+K}} L_k^{(K-1)}\left(\frac{-n_s}{N(1+N)}\right) e^{-n_s/(1+N)}$$

for $k = 0, 1, 2, \ldots$, where $L_k^{(K-1)}$ is the Laguerre polynomial of order k and $n_s = \bar{n}_s/p$, the mean signal count in a pulsed slot.

Let $n_b = KN$. In the limit of large K with n_b fixed, the photon counting statistics approach the Poisson,

$$p_0(n;K) \xrightarrow[K\to\infty]{} \frac{n_b^n e^{-n_b}}{n!} \tag{9}$$
$$p_1(n;K) \xrightarrow[K\to\infty]{} \frac{(n_b+n_s)^n e^{-(n_b+n_s)}}{n!} \tag{10}$$

In practice, it is common that $K \gg 1$, and a Poisson channel model is used. Let us suppose the Poisson approximation holds, such that the channel is defined by (9),(10). Let $i_p^{\text{OOK}}(n_b)$ be the PIE of the Poisson OOK channel with mean n_b noise counts per slot. Then we have [17]

$$i_p^{\text{OOK}}(n_b) \geq (1 + n_b/n_s)\log_2(1 + n_s/n_b) - 1/\ln(2) - \frac{1}{n_s}$$

which is increasing with n_s at large n_s. Hence arbitrarily large PIE can be achieved on the noisy Poisson OOK channel. Presuming the conjectured Holevo limit, (6), holds, we have a contradiction, and hence the Poisson approximation cannot hold at large PIE for any finite K.

[2] We note that the asymptotic approximation (8) is *equal* to the asymptotic formula for pulse-position modulation (PPM) and ideal photon counting [8], confirming the well-known result that the efficiencies of PPM and OOK agree at large PIE.

1) Poisson channel c_d at large i_p: It is, nonetheless, instructive to investigate the behavior of the noisy Poisson OOK channel at large i_p. At large PIE the noisy Poisson OOK channel bounds and is well approximated by the noisy Poisson PPM channel. Let i_p^{PPM} and i_d^{PPM} be the PIE and DIE of the order M noisy Poisson PPM channel, and

$$c_d^{\text{PPM}}(i_p) = \max_{M, n_s | i_p^{\text{PPM}} = i_p} i_d^{\text{PPM}}$$

Define the functions

$$\tilde{i}_p = \frac{\log_2(M^*)(1 - e^{-n_s^*})}{n_s^*}$$
$$\tilde{c}_d = \tilde{i}_p n_s^* / M^*$$

where (n_s^*, M^*) satisfy

$$(n_s^* + n_b)\ln(1 + n_s^*/n_b) - n_s^* = \ln(M^*)(1 - e^{-n_s^*})$$

Then for any pair $(i_p^{\text{PPM}}, c_d^{\text{PPM}})$, there exists a pair $(\tilde{i}_p, \tilde{c}_d) \geq (i_p^{\text{PPM}}, c_d^{\text{PPM}})$ [17]. Hence c_d^{PPM} grows no faster in i_p^{PPM} than $\tilde{c}_d$. At large $\tilde{i}_p$ we have

$$\begin{aligned}\tilde{c}_d \approx & n_b \tilde{i}_p \exp(\tilde{i}_p \ln(2) + 1) \times \\ & \exp\left(\frac{-n_b \tilde{i}_p \ln(2) \exp(\tilde{i}_p \ln(2) + 1)}{1 - \exp(-n_b \exp(\tilde{i}_p \ln(2) + 1))}\right)\end{aligned}$$

and, although $\tilde{i}_p$ is not strictly bounded, $\tilde{c}_d$ falls off as $e^{-e^{\tilde{i}_p}}$ at large $\tilde{i}_p$, so that it is impractical to achieve large PIE on the noisy Poisson OOK channel.

V. OOK WITH SINGLE-PHOTON SHUTOFF

We now consider a modification of conventional OOK with ideal photon counting in the absence of background. Recall that on this channel the detection of a single photon is sufficient to unambiguously resolve the transmitted symbol. Any additional detection events convey no more information. Hence, if the transmitter knew the instant a photon were detected at the receiver, it could stop transmitting the current symbol, reducing the photon cost, with no change to the channel capacity. A modified—and idealized—receiver structure that performs this operation is illustrated in Fig. 3, in which the receiver provides delay- and noise-free feedback to the transmitter, informing it to terminate the transmitted pulse as soon as the first photon is detected. If no photons are detected, either because vacuum was transmitted or because an erasure event occurred, the receiver waits until the end of the T-second window and then restarts anew. We refer to this system as *OOK with single-photon shutoff* and use the shorthand notation 1S in referring to its variables in the following analysis.

For this receiver architecture, the channel is still given by the Z channel of Fig. 2. Hence the mutual information between the input and output does not change, but now the mean photon number per channel use has been reduced to

$$\bar{n}^{1\text{S}} = p\lambda E[\tau] = p(1 - e^{-\lambda T}) = \frac{\bar{n}^{\text{OOK}}}{d(\epsilon)}$$

where τ is the random duration of a pulse, $\bar{n}^{\text{OOK}} = p\lambda T$ is the mean photon number of conventional OOK. Hence the single photon shutoff system requires a factor $d(\epsilon)$ fewer photons than conventional OOK with the same (p, ϵ).

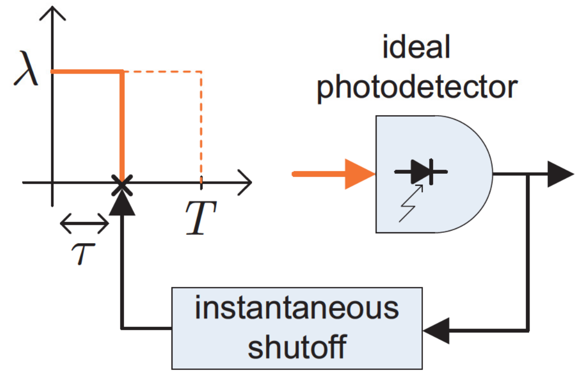

Fig. 3. An ideal single-photon shutoff receiver, with feedback to the transmitter.

The OOK single-photon shutoff system achieves this increase in photon efficiency at a price of requiring additional resources for the feedback channel and increased bandwidth usage on the forward (optical) link. Here we limit our focus to the bandwidth increase in the forward link, which results from shortened average pulse durations.

The single-photon shutoff OOK pulse train consists of a sequence of modulated pulses of random duration. The power spectral density of the process is given by [15]

$$\begin{aligned}S(f) = & \frac{p\lambda^2 T}{(\lambda T)^2 + (2\pi f T)^2}\Bigg(2 - 2\lambda T e^{-\lambda T}\text{sinc}(2\pi f T) \\ & - (2 - 2p)e^{-\lambda T}\cos(2\pi f T) - p - pe^{-2\lambda T} \\ & + p(1-p)^2 \sum_{k=-\infty}^{\infty} \delta(fT - k)\Bigg)\end{aligned}$$

where $\text{sinc}(x) \equiv \sin(x)/x$. Fig. 4(a) illustrates the power spectral density for various λT, assuming $p \ll 1$, which is valid for PIE $\gg 1$. In Fig. 4(b) we have plotted the mean photon flux contained in $|f| < \lambda/(1 - e^{-\lambda T})$ as a function of λT, which shows that to a very good approximation 90% of the total mean photon flux is contained within this frequency band. This follows heuristically, as the reciprocal of the average duration of a pulse at large λT is approximately $1/E[\tau] = \lambda/(1 - e^{-\lambda T})$. In the remainder we take $1/E[\tau] = \lambda/(1 - e^{-\lambda T})$ to be the bandwidth of the single-photon shutoff OOK scheme. This is also consistent with the treatment of conventional OOK with pulse duration T, wherein 90% of the mean photon flux is concentrated in a frequency bandwidth of $1/T$.

Given the bandwidth definition, the number of temporal dimensions per channel use—determined by the time-bandwidth product—is given by

$$d^{1\text{S}} = \frac{\lambda T}{1 - e^{-\lambda T}} = \frac{-\ln(1 - \epsilon)}{\epsilon} = d(\epsilon)$$

Hence the photon and dimensional efficiencies of the single-

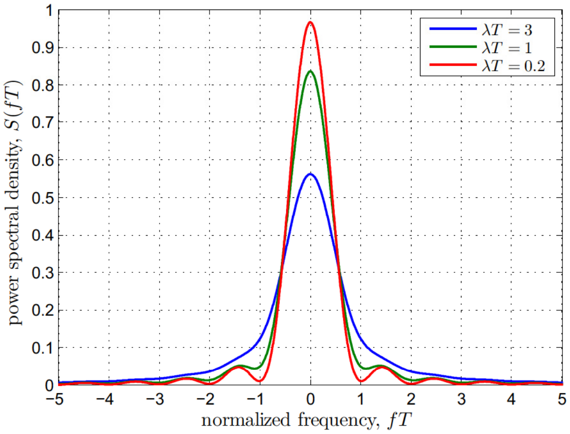

(a)

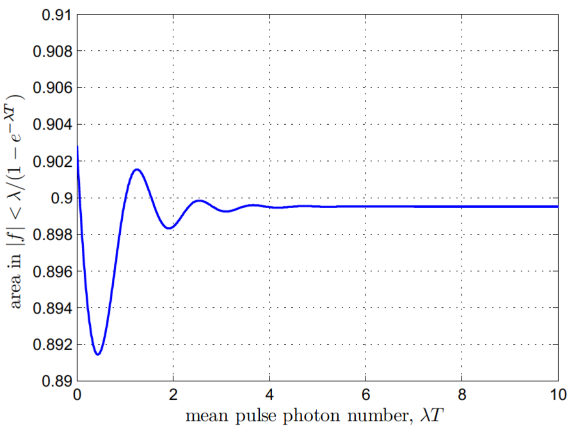

(b)

Fig. 4. Power spectral density of OOK with single-photon shutoff assuming $p \ll 1$ (a) The power spectral density plotted in terms of the normalized frequency variable fT. (b) The area underneath $S(f)$ for $|f| \leq \lambda/(1 - e^{-\lambda T})$.

photon shutoff OOK system are

$$i_p^{1S} = h_2(\bar{n}) - h_2(\epsilon)$$
$$i_d^{1S} = \frac{\bar{n}}{d(\epsilon)}\left[h_2(\bar{n}) - h_2(\epsilon)\right] = \frac{\bar{n}}{d(\epsilon)} i_p^{1S}$$

Comparing these expressions to the corresponding ones for conventional OOK, we have

$$\frac{i_d^{\text{OOK}}}{i_d^{1S}} = \frac{i_p^{1S}}{i_p^{\text{OOK}}} = d(\epsilon)$$

i.e., for the same channel transition probability ϵ and input probability p, the modified OOK system with single-photon shutoff has an increase in PIE by a factor of $d(\epsilon)$ and a decrease in DIE by the same factor, relative to conventional OOK. This is a favorable tradeoff when the log-domain curve defined by the pair of points $(\log_2 i_p^{\text{OOK}}, \log_2 i_d^{\text{OOK}})$ has slope less than -1. This occurs approximately at

$$i_p^* \approx 2\log_2 e / d(\epsilon) < 2\log_2 e \qquad (11)$$

Hence when $i_p > 2\log_2 e \approx 2.885$ bits/photon, single-photon shutoff offers a favorable tradeoff between bits per photon and bits per dimension.

Let

$$c_d^{1S}(i_p) = \max_{\bar{n}, \epsilon \in [0,1]} i_d^{1S} \qquad (12)$$

A numerical evaluation of (12) is illustrated in Fig. V, showing that OOK with single-photon shutoff yields DIE better than conventional OOK when the PIE exceeds 2.22 bits/photon, consistent with (11). The performance degradation at low PIE is due to the high mean photon number in this regime. When $\lambda T \gg 1$, most pulses are terminated before the slot duration ends and the information rate is near its ideal limit of 1 bit per channel use. Consequently, the increase in the bandwidth due to the premature termination of the pulse is not matched by an equivalent increase in mutual information, causing a degradation in the DIE relative to standard OOK.

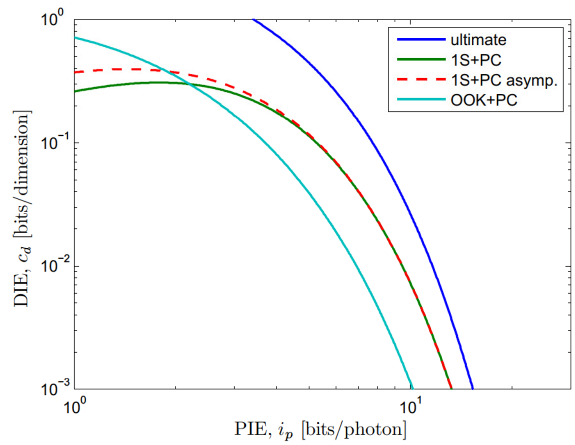

Fig. 5. The (PIE,DIE) pairs for the Holevo bound (ultimate) (2), conventional OOK with photon counting (OOK+PC) (7), OOK with single-photon shutoff (1S+PC) (12), and its asymptotic approximation (1S+PC asymp.)(V)

At large i_p, we have [15]

$$i_D^{1S} \approx \left(e\, i_p\, 2^{-i_p}\right)\left[\frac{2^{-h_2(\epsilon)}}{d(\epsilon)}\right]$$

The factor in the square brackets is a function of ϵ but not of the photon efficiency i_p. Hence the optimum ϵ is *independent* of the photon efficiency when $i_p \gg 1$:

$$\epsilon^* = \arg\max_{\epsilon \in [0,1]} 2^{-h_2(\epsilon)}/d(\epsilon) \approx 0.876$$

yielding

$$c_d^{1S} \approx 0.274 c_d^{\text{Hol}} \qquad (13)$$

at large i_p. Hence feedback not only enables higher DIE than otherwise possible with conventional OOK, but also yields a DIE which has the same parametric dependence as the Holevo bound.

In the large i_p regime ($i_p \gtrsim 4$ bits/photon), the optimal ϵ^* yields an erasure probability of $(1 - \epsilon^*) \approx 0.124$, which corresponds to $\lambda T \approx 2.087$. That is, the optimal photon flux at high PIE would cost 2.087 photons per pulse if the transmission continued for the entire symbol duration T. The single-photon shutoff strategy reduces the mean photon cost to $\bar{n} \approx 0.876$ at the expense of an increase in spectral occupancy by a factor of $d(\epsilon^*) \approx 2.383$. The net DIE improvement from this tradeoff, however, is significant. Unlike conventional OOK, the asymptotic dimensional efficiency of OOK with single-photon shutoff has the *same* parametric dependence as the optimal Holevo bound. In particular, its asymptotic DIE is inferior to the ultimate quantum limit by a constant multiplicative factor of 0.274, whereas conventional OOK's asymptotic DIE is inferior to the ultimate quantum limit by a factor that increases linearly in i_p.

VI. OOK WITH SINGLE-PHOTON NUMBER STATES

Recall that the single-mode channel reduces to a beamsplitter of transmissivity η. In the limit that $\eta = 1$, the Holevo capacity can be achieved by transmitting a number-state alphabet $\{|n\rangle : n = 0, 1, \dots\}$ with a geometric distribution $p(n) = n_S^n/(1+n_S)^{n+1}$, where n_S is the mean photon number, and receiving the signal with an ideal photon-counting receiver [18]. When $n_S \ll 1$, the binary alphabet $\{|0\rangle, |1\rangle\}$ suffers only a small loss relative to the Holevo limit. Here we consider the performance of this binary number-state system, and examine the degradation in a near-field communication system wherein $\eta \approx 1$ holds for multiple modes.

Let the transmitter transmit $|1\rangle$ with probability p and $|0\rangle$ with probability $1-p$. When the transmitter field mode is in the vacuum state, $|0\rangle$, then the output of the beamsplitter is also in a vacuum state. When the transmitter field mode is in the number state $|1\rangle$, then the output field mode is in a mixed state $\eta|1\rangle\langle 1| + (1-\eta)|0\rangle\langle 0|$. Hence, an ideal photon counting photodetector will yields conditional output probabilities

$$\Pr\big(\text{count} = 1 \big| |1\rangle \text{sent}\big) = \eta$$
$$\Pr\big(\text{count} = 0 \big| |1\rangle \text{sent}\big) = 1-\eta$$

and the channel reduces to a Z-channel, with crossover probability $1-\eta$, illustrated in Fig. 6. We denote variables pertaining to this architecture with the superscript 1NS.

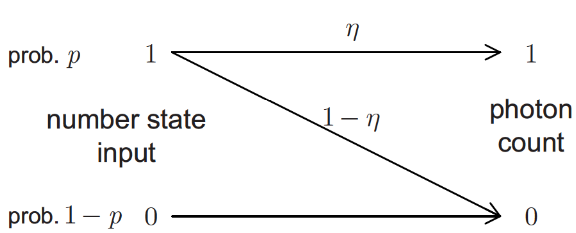

Fig. 6. The erasure channel that defines communication with the number-state binary alphabet $\{|0\rangle, |1\rangle\}$.

It follows that i_p^{1NS} and i_d^{1NS} are identical to their counterparts in (coherent-state) OOK with single-photon shutoff, but with ϵ replaced by the channel transmissivity η. That is, the photon and dimensional efficiencies per (detected) photon are given by

$$\begin{aligned} i_p^{\text{1NS}} &= h_2(\bar{n}) - h_2(\eta) \quad \text{bits/photon} \\ i_d^{\text{1NS}} &= \bar{n}[h_2(\bar{n}) - h_2(\eta)] \\ &= h_2^{-1}\big(i_p + h_2(\eta)\big) i_p \quad \text{bits/dimension,} \end{aligned} \tag{14}$$

where $\bar{n} \equiv p\eta$ is the probability that a photon is counted by the receiver. Note that we normalize by the mean number of *detected* photons, to be consistent with our prior definitions of photon efficiency.

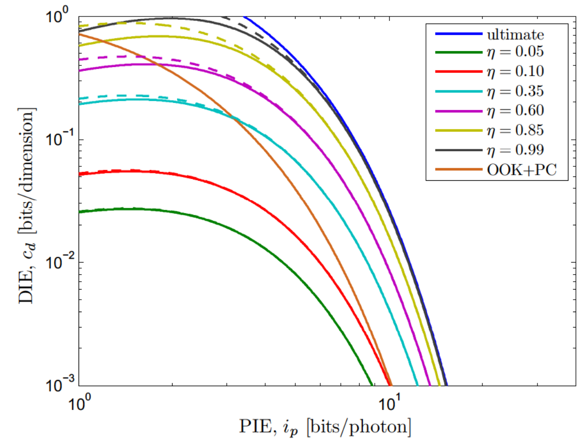

(a)

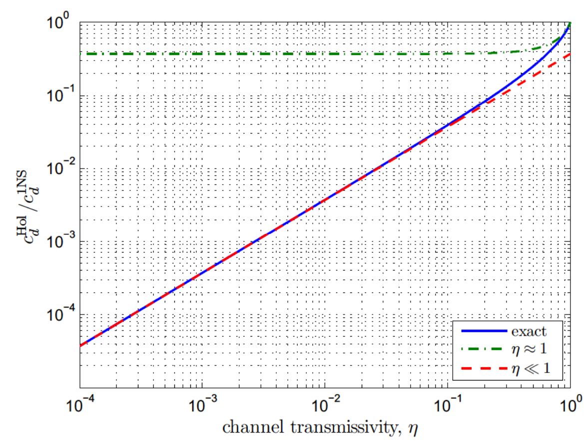

(b)

Fig. 7. The numerically-evaluated DIE curve for OOK with single-photon number states and ideal photon counting, as well as its asymptotic approximation at large PIE, are plotted for several different η. (a) The numerically-evaluated PIE versus DIE tradeoff curves (solid lines) and their asymptotic approximations (dashed lines) at different η. The Holevo bound, and the PIE-DIE curves for conventional OOK with ideal photon-counting (OOK+PC) are also plotted for comparison. (b) The $c_d^{\text{Hol}}/c_d^{\text{1NS}}$ ratio for $i_p \gg 1$, at different η. Dashed (red) line and dash-dotted (green) line denote asymptotic approximations.

From (14), we see that fixing (η, i_p) fixes i_d^{1NS}, hence $c_d^{\text{1NS}}(i_p;\eta) \equiv i_d^{\text{1NS}}(i_p,\eta)$. Fig. 7(a) illustrates the pairs $(i_p^{\text{1NS}}, c_d^{\text{1NS}})$ for several values of η. The slope of c_d^{1NS} at large i_p is greater than that of c_d^{OOK}, hence, for every $\eta > 0$, there exists an $i_p^*(\eta)$, such that for all $i_p > i_p^*(\eta)$, $c_d^{\text{1NS}}(i_p;\eta) > c_d^{\text{OOK}}(i_p)$. However, $i_p^*(\eta)$ increases with decreasing η.

For $i_p \gg 1$ we have

$$c_d^{\mathrm{1NS}}(i_p;\eta) \approx (e i_p 2^{-i_p}) 2^{-h_2(\eta)} \approx c_d^{\mathrm{Hol}} 2^{-h_2(\eta)} \tag{15}$$

Hence, as with OOK with single-photon shutoff, OOK with single-photon number states achieves the *same* parametric dependence as the ultimate efficiency, with a constant penalty factor. In the OOK with single-photon shutoff scheme, that penalty is roughly constant at large i_p. Here the penalty is a function of the channel transmissivity, $2^{-h_2(\eta)}$, which is approximately equal to $(1-\eta)^{1-\eta}/e^{1-\eta}$ for $\eta \approx 1$, and approximately equal to η/e for $\eta \ll 1$. Figure 7(b) shows the variation of this constant factor as a function of η, along with the aforementioned asymptotes. From Eqs. (13) and (15), we see that at $\eta \approx 0.534$, the two schemes achieve the same large i_p asymptote.

Since the efficiency of the single-photon number-state OOK modulation is determined by the channel losses, we briefly discuss typical power coupling that can be achieved in a near-field link geometry. The normal-mode decomposition for hard circular apertures gives rise to Prolate-spheroidal eigenfunctions [19], and singular values that are not in closed form. This is no longer the case if we replace the hard-pupil apertures of the transmitter and receiver with Gaussian soft apertures [20]. In particular, it can be shown that the input and output eigenfunctions are Laguerre-Gaussian functions, and there are m degenerate eigenvalues equal to $\eta_m = \eta_0^m$ for $m = 1, 2, \ldots$, where

$$\eta_0 = \frac{1 + 2D_F - \sqrt{1 + 4D_F}}{2D_F}$$

As an example, a near-field system with $\lambda_0 = 1\mu$m, $L = 1$km, and equal-size soft Gaussian transmitter and receiver apertures with e^{-1} amplitude attenuation radius equal to 0.1m has a $D_F = 250$ [3] For this case, the first 55 eigenvalues are greater than 0.5, and the top 200 eigenvalues are greater than 0.28.

VII. Discussion

It is well known that the Holevo information limits may be approached by encoding information in a coherent-state alphabet, which at high photon information efficiencies is well-approximated by a binary modulation, such as OOK. However, we know only the behavior of the required corresponding measurement on the optical codewords generated by this encoding–no explicit receiver architecture is know for a Holevo-bound-achieving measurement.

The state of the art realization of high PIE optical communication is generalized OOK (implemented as high-order PPM) in conjunction with a photon-counting receiver. In the absence of background the DIE achievable with this scheme is inferior to the Holevo limit by a factor that grows linearly with the PIE. A commonly assumed Poisson approximation to the photon-counting measurement In the presence of multimode background noise must be inaccurate at large PIE for any number of noise modes, as it predicts unbounded PIE while the (conjectured) Holevo limit is bounded. However, although not strictly bounded, the Poisson OOK channel in noise has a DIE that falls off doubly exponentially in PIE, such that, for most practical purposes, large PIE on the noisy Poisson OOK channel is also not achievable.

We investigated two methods to extend the efficiencies achievable *with* a photon-counting receiver in the absence of background noise. Each significantly improves on conventional OOK at large PIE and achieves the same parametric dependence as the Holevo limit, such that the degradation is a constant factor relative to the Holevo limit at large PIE. However, they each, as presented, require assumptions the would make a practical implementation challenging.

The first approach, OOK with single-photon shutoff, as presented requires a perfect feedback channel with no latency. Incorporating a finite delay in the feedback channel is straightforward, but may limit the feasibility to scenarios where the latency is a small fraction of the slot width. Moreover, we assess no cost to the feedback channel. Although this is consistent insofar as one typically doesn't assess a power cost due to operations at the receiver, it may not reflect the practical issues related to establishing a feedback channel. While it is apparent that all of these issues are pertinent to realizing a communication system with the feedback, they should not overshadow the underlying fundamental insight offered by this feedback architecture: the asymptotic suboptimality of OOK plus photon-counting in DIE is fundamentally due to energy transmission that does not contribute to information transfer once a photon is detected at the receiver. If the transmitter could shutoff, via some ideal feedback or an oracle, at the instant at which the receiver detects the first photon in a slot, the energy conserved from shutting off the transmitter is sufficient to achieve a DIE $c_d^{\mathrm{1S}} = 0.274 c_d^{\mathrm{Hol}}$, which is suboptimal by the constant factor 0.274.

The second approach we considered requires one to transmit number states, $\{|0\rangle, |1\rangle\}$, rather than coherent states. Unlike coherent-state modulation, this architecture inherently pushes the complexity to the transmitter by requiring on-demand generation of a (nonclassical) single-photon number state in a defined spatiotemporal and polarization mode, in addition to requiring efficient transfer of this state from the transmitter to the receiver. Nevertheless, if such a source were available, the DIE is asymptotically $c_d^{\mathrm{1NS}} = 2^{-h_2(\eta)} c_d^{\mathrm{Hol}}$, which is also suboptimal by only a constant factor $2^{-h_2(\eta)}$. This factor now depends on the efficiency, η, with which the number state is transmitted to the photodetector, where η refers to the aggregate efficiency of transmitting a number state, including transmitter optical losses, diffraction loss and absorption, the receiver optical efficiency, and the photodetector quantum efficiency. Although this scheme will always perform superior to standard OOK at high enough PIE, the crossover point moves out to higher values of PIE as η degrades. As a rule of thumb, if $\eta > 0.1$, the crossover point is at approximately

[3] The Fresnel number product D_F, in Eq. (1), depends on the aperture area. For a soft Gaussian aperture $A(\boldsymbol{\rho}) \equiv e^{-|\boldsymbol{\rho}|^2/r^2}$, where $\boldsymbol{\rho}$ is the 2D spatial coordinate vector on the aperture plane and r is the e^{-1}-attenuation radius, the effective aperture area is given by $\int A^2(\boldsymbol{\rho})\mathrm{d}\boldsymbol{\rho} = \pi r^2/2$.

PIE $= 10$ bits/photon. Achieving 10% system transmission efficiency, including all of the aforementioned factors, is in general not trivial. However, with improving device technologies it may become feasible to achieve such efficiency values. It is also worthwhile to point out that single-photon number-state generation is an active area of research that has produced several approaches to date, some of which are better suited than others for high-PIE optical communication applications [21].

ACKNOWLEDGMENT

The research described in this publication was supported by the DARPA InPHo program under contract JPL 97-15402, and the JPL R&TD Program, and was carried out by the Jet Propulsion Laboratory, California Institute of Technology, under a contract with the National Aeronautics and Space Administration

REFERENCES

[1] M. A. Nielsen and I. L. Chuang, *Quantum Computation and Quantum Information*. Cambridge: Cambridge Univ., 2000.

[2] J. Lesh, J. Katz, H. Tan, and D. Zwilliinger, "2.5-bit/detected photon demonstration program: Description, analysis, and phase I results," *TDA Progress Report*, vol. 42–66, pp. 115–132, September 1981.

[3] B. Robinson, D. Caplan, M. Stevens, R. Barron, E. Dauler, and S. Hamilton, "1.5-photons/bit photon-counting optical communications using geiger-mode avalanche photodiodes," in *LEOS Summer Topical Meetings, 2005 Digest of the*, July 2005, pp. 41–42.

[4] E. Dauler, B. Robinson, A. Kerman, V. Anant, R. Barron, K. Berggre, D. Caplan, J. Carney, S. Hamilton, K. Rosfjord, M. Stevens, and J. Yang, "1.25-Gbit/s photon-counting optical communications using a two-element superconducting nanowire single photon detector," in *Proceedings of the SPIE*, vol. 6372, October 2006.

[5] B. S. Robinson, A. J. Kerman, E. A. Dauler, D. M. Boroson, S. A. Hamilton, J. K. W. Yang, V. Anant, and K. K. Berggren, "Demonstration of gigabit-per-second and higher data rates at extremely high efficiency using superconducting nanowire single photon detectors," in *Proceedings of the SPIE*, vol. 6709, San Diego, CA, Aug. 2007.

[6] K. Birnbaum, W. Farr, J. Gin, B. Moision, K. Quirk, and M. Wright, "Demonstration of a high-efficiency free-space optical communications link," in *Proceedings of the SPIE*, vol. 7199, January 2009.

[7] S. Guha, "Structured optical receivers to attain superadditive capacity and the Holevo limit," *Phys. Rev. Lett.*, vol. 106, p. 240502, 2011.

[8] S. Dolinar, K. Birnbaum, B. Erkmen, and B. Moision, "On approaching the ultimate limits of photon-efficient and bandwidth-efficient optical communication," in *Space Optical Systems and Applications (ICSOS), 2011 International Conference on*, May 2011, pp. 269 –278.

[9] B. I. Erkmen, K. M. Birnbaum, B. E. Moision, and S. J. Dolinar, "The Dolinar receiver in an information theoretic framework," *Proc. SPIE*, vol. 8163, p. 81630U, 2011.

[10] J. H. Shapiro, "The quantum theory of optical communications," *IEEE J. Sel. Top. Quantum Electron.*, vol. 15, p. 1547, 2009.

[11] ——, "Corrections to "the quantum theory of optical communications" [Nov/Dec 09 1547-1569]," *IEEE J. Sel. Top. Quantum Electron.*, vol. 16, p. 698, 2010.

[12] ——, "Normal-mode approach to wave propagation in the turbulent atmosphere," *Appl. Opt.*, vol. 13, pp. 2614–2619, 1974.

[13] V. Giovannetti, S. Guha, S. Lloyd, L. Maccone, J. H. Shapiro, B. J. Yen, and H. P. Yuen, "Classical capacity of free-space optical communication," *Quantum Inf. Comput.*, vol. 4, pp. 489–499, 2004.

[14] V. Giovannetti, S. Guha, S. Lloyd, L. Maccone, and J. H. Shapiro, "Minimum output entropy of bosonic channels: a conjecture," *Phys. Rev. A*, vol. 70, p. 032315, 2004.

[15] B. I. Erkmen, B. E. Moision, S. J. Dolinar, K. M. Birnbaum, and D. Divsalar, "On approaching the ultimate limits of communication using a photon-counting detector," in *Proceedings of the SPIE*, San Francisco, CA, January 2012.

[16] R. M. Gagliardi and S. Karp, *Optical Communications*, 1st ed. New York: John Wiley & Sons, 1976.

[17] B. Moision, B. Erkmen, W. Farr, S. Dolinar, and K. Birnbaum, "Limits on achievable dimensional and photon efficiencies with intensity-modulation and photon-counting due to non-ideal photon-counter behavior," in *Proceedings of the SPIE*, San Jose, CA, Jan 2012.

[18] H. P. Yuen and M. Ozawa, "Ultimate information carrying limit of quantum systems," *Phys. Rev. Lett.*, vol. 70, pp. 363–366, 1993.

[19] D. Slepian, "Analytic solution of two apodization problems," *J. Opt. Soc. Am.*, vol. 55, pp. 1100–1115, 1965.

[20] J. H. Shapiro, S. Guha, and B. I. Erkmen, "Ultimate channel capacity of free-space optical communications [invited]," *J. Opt. Netw.*, vol. 4, pp. 501–516, 2005.

[21] M. D. Eiseman, J. Fan, A. Migdall, and S. V. Polyakov, "Invited review article: Single-photon sources and detectors," *Rev. Sci. Instrum.*, vol. 82, p. 071101, 2011.